ADVANCED MATERIALS INTERFACES
www.advmatinterfaces.de

Localized and Surface Plasmons Coupling for Ultrasensitive Dopamine Detection by means of SPR-Based Perylene Bisimide/Au Nanostructures Thin Film

Rosanna Pagano, Zois Syrgiannis, Simona Bettini, Chiara Ingrosso, Ludovico Valli, Gabriele Giancane,* and Maurizio Prato*

Dopamine (DA) is an important catecholamine neurotransmitter involved in neural and hormonal functions. Neural diseases, as Parkinson's, are connected to a significant lowering of DA concentration to picomolar levels in cerebrospinal fluid. So, in this contribution, a hybrid active layer based on a perylene bisimide (PBI) derivative and multishaped Au nanostructures is proposed for the development of surface plasmon resonance (SPR) dopamine detection system. PBI molecules, transferred as thin film by the dip coating approach, are demonstrated to be able to detect dopamine down to 10^{-12} M by SPR method. The presence of Au nanostructures promotes an important surface enhanced Raman scattering effect of Raman PBI signals highlighting a strong energetic communication between the two species. In this way, when PBI/Au nanostructures (AuNS) films are deposited by the layer-by-layer method and used for DA SPR detection, the sensitivity toward dopamine 10^{-12} M is doubled. The PBI/AuNS hybrid layer is able to detect picomolar concentration of dopamine, due to the coupling of localized (AuNS) and propagating surface plasmons on SPR slide. In particular, an interfacial coupling among localized surface plasmon resonance on AuNS and the propagating plasmon on Au thin film (of SPR slide) can be promoted.

1. Introduction

Dopamine (DA) is one of the most important catecholamines largely diffuse in human brain and biological fluids (saliva, blood, serum, urine).[1–3] Catecholamines, including DA, noradrenaline, levodopa, norepinephrine, serotonin are fundamental neurotransmitters governing neural communication, as well as vascular and hormone functions.[4,5] DA levels analysis in biological complex fluids, especially cerebrospinal fluid (CSF), is an intriguing challenge to perform an early diagnosis of several neural diseases and then therapeutic treatments.[6–8] Parkinson's, Huntington's, Alzheimer's diseases, Schizophrenia, epilepsy, and memory loss are some of the widespread neural sicknesses related to DA down-level in the CSF.[8–10] In healthy patients, DA CSF levels are reported to be in the 0.5×10^{-9} to 25×10^{-9} M concentration range,[11] whilst, in Parkinson's disease affected people, DA CSF levels drop down to sub-nanomolar concentration (below 100×10^{-12} M). [12,13]

In the last years, in order to reply to the demand of ultrasensitive DA detection in biological fluids, as CSF or sera, the researchers' interest in innovative optical and spectroscopic sensing systems, especially based on surface enhanced Raman scattering (SERS) and surface plasmon resonance (SPR) methods, has been constantly rising.[14–17] In fact,

R. Pagano, S. Bettini, L. Valli
Department of Biological and Environmental Sciences and Technologies
DISTEBA
University of Salento
Via per Arnesano, Lecce 73100, Italy
E-mail: simona.bettini@unisalento.it

The ORCID identification number(s) for the author(s) of this article can be found under https://doi.org/10.1002/admi.202101023.

[+]Present address: Simpson Querrey Institute, Northwestern University, Chicago, IL 60611, USA and Department of Chemistry, Northwestern University, Evanston, IL 60208, USA

DOI: 10.1002/admi.202101023

Z. Syrgiannis,[+] M. Prato
Department of Chemical and Pharmaceutical Sciences
University of Trieste
via L. Giorgieri 1, Trieste I-34127, Italy

C. Ingrosso
CNR-IPCF Istituto per i Processi Chimico-Fisici
Sez. Bari, c/o Dip. Chimica Via Orabona 4, Bari 70126, Italy

G. Giancane
Department of Cultural Heritage
University of Salento
Via D. Birago, Lecce 73100, Italy
E-mail: gabriele.giancane@unisalento.it

M. Prato
Center for Cooperative Research in Biomaterials (CIC biomaGUNE)
Basque Research and Technology Alliance (BRTA)
Paseo de Miramón 182, Donostia San Sebastián E-20014, Spain

M. Prato
Basque Foundation for Science
Ikerbasque, Bilbao E-48013, Spain

spectroscopic techniques, in general, in contrast to classical approaches devoted to DA detection and quantification, as chromatographic methods, do not require complicated and sophisticated instruments or sample pretreatment being, indeed, less time-consuming.[18] Considering the low sensitivity typical of this kind of techniques, many efforts have been devoted to the implementation and the optimization of the active layer/transducer for DA detection at least down to the physiological concentration.[19–21] With this aim, in this work, an SPR transducer has been ad hoc designed and developed in order to gain sub-nanomolar DA recognition even in complex matrix, as artificial CSF (aCSF). An amphiphilic perylene bisimide derivative bearing a positive charge (perylene bisimide, PBI, **Figure 1**) has been used for anchoring citrate-capped Au nanostructures, through the layer-by-layer (LbL) method, onto solid supports including SPR slides.

PBI was chosen as a component of the hybrid proposed surface functionalization due to its well-known capability of spectroscopic sensing of biological interesting aromatic amines at trace levels.[22] In fact, the wide π-delocalization, the intense absorption and emission features, the presence of electron withdrawing groups (the imides), the potentiality to govern their aggregation state (as H or J aggregation) both in solution and onto solid thin films have proposed these systems, in the last decade, as very promising for the development of spectroscopic sensors[22–24] In our previous work,[22] we have already demonstrated the capabilities to detect aromatic biogenic amines down to 10^{-10} M thorough SPR approach by using a differently functionalized perylene bisimide derivative. In the present work, we have further optimized the PBI-based layer using the amphiphilic derivative reported in Figure 1. It allows avoiding both the use of the polyelectrolyte anchors and the generation of electrostatic interactions in order to transfer the ad hoc synthetized Au nanostructures (AuNS). [25] The coupling of the localized and the surface plasmons[26,27] permits us to achieve high sensitivity, down to DA picomolar concentration in aCSF, which is, if compared with the literature,[14,17] a very promising result for the further development of an SPR sensor for DA detection in real physiological fluids.

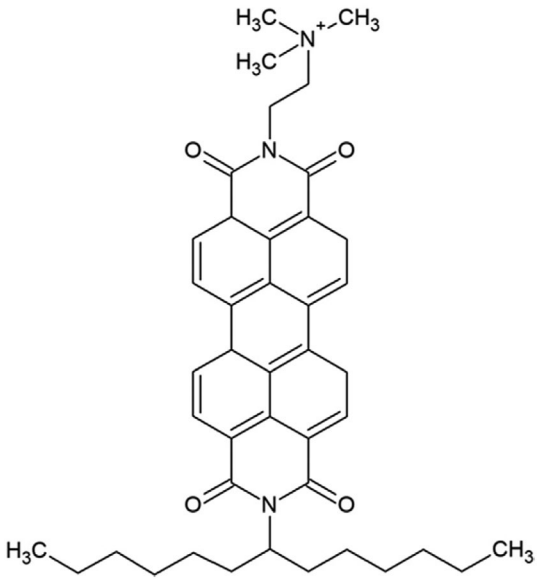

Figure 1. Chemical structure of PBI derivative synthetized in this work, as reported in the Supporting Information, and used for the realization of the hybrid layers with Au nanostructures.

2. Results and Discussion

2.1. Morphological and Spectroscopic Characterizations

The citrate-capped Au NS were morphologically investigated by means of transmission electron microscopy (TEM, **Figure 2**a; Figure S1, Supporting Information). The TEM images show that the AuNS grow with a polydisperse morphology, relaying mostly in populations of triangular-shaped nanoparticles, 40.2 ± 21.9 nm in edge, and of nanospheres, 34.5 ± 11.7 nm in size(Figure 2b,c), according to literature.[28] In addition, lower populations of pentagonal-shaped nanoparticles, 22.6 ± 3.1 nm in edge (Figure S1a–c, Supporting Information), and of nanorods, 100.9 ± 60.1 nm in length and 29.5 ± 10.3 nm in diameter (Figure S1b,d, Supporting Information), as well as larger aggregated nanostructures having an irregular geometry, are observed (Figure S1b, Supporting Information).

XRD profile (Figure 2d) is characterized by the presence of four peaks centered at 38.1°, 44.3°, 64.5°, and 77.7° corresponding to the Au face center cubic lattice.[29] The most intense diffraction peak located at 38.1° suggests that zero valent Au preferentially grows along the (111) direction.[28,30]

UV–vis absorption spectrum of the colloidal suspension in ultrapure water of the as-synthetized AuNS shows a broad maximum centered at 535 nm (**Figure 3**a). The heterogenous AuNS with different shape and size promote the formation of a broad signal due to the superposition of plasmon resonances of spherical, triangular and rod-like Au nanostructures.[31] The contribute of the smallest spherical-shaped AuNS to plasmonic peak is located at about 530 nm[32] and the contributes of the biggest spherical AuNS are red-shifted and influenced by scattering events (Figure S2, Supporting Information). A broadening effect of the UV–vis spectrum of AuNS is due to the presence of triangular and pentagonal gold nanostructures. A more accurate study of the symmetry of the AuNS plasmon peak suggests indeed the presence of three different signals (Figure S2, Supporting Information) located at 535, 590, and 615 nm. The principal plasmon band position agrees with a main AuNS population based on spherical and triangular shaped nanoparticles whilst the other red-shifted contributes should be related to anisotropic and larger nanostructures,[33] in perfect agreement with TEM analysis.

FTIR performed on the AuNS evidences the presence of the capping agent (Figure 3b): the AuNS IR spectrum exhibits all the most prominent signals of citric acid. At 1720 cm^{-1} the stretching mode of C=O (C(O) −OH) can be identified and the O−H in-plane bending is located at 1402 cm^{-1}. The signal at 1583 cm^{-1} emerges only in the FTIR spectrum of the citrate-capped gold nanostructures: such a band can be attributed to the asymmetric stretching of the carboxylate group, indicating the metal-coordination by the deprotonated carboxylic group.[34] The symmetric and asymmetric modes of C−O−H in the range of 1276–1150 cm^{-1} are influenced by the presence of the metallic

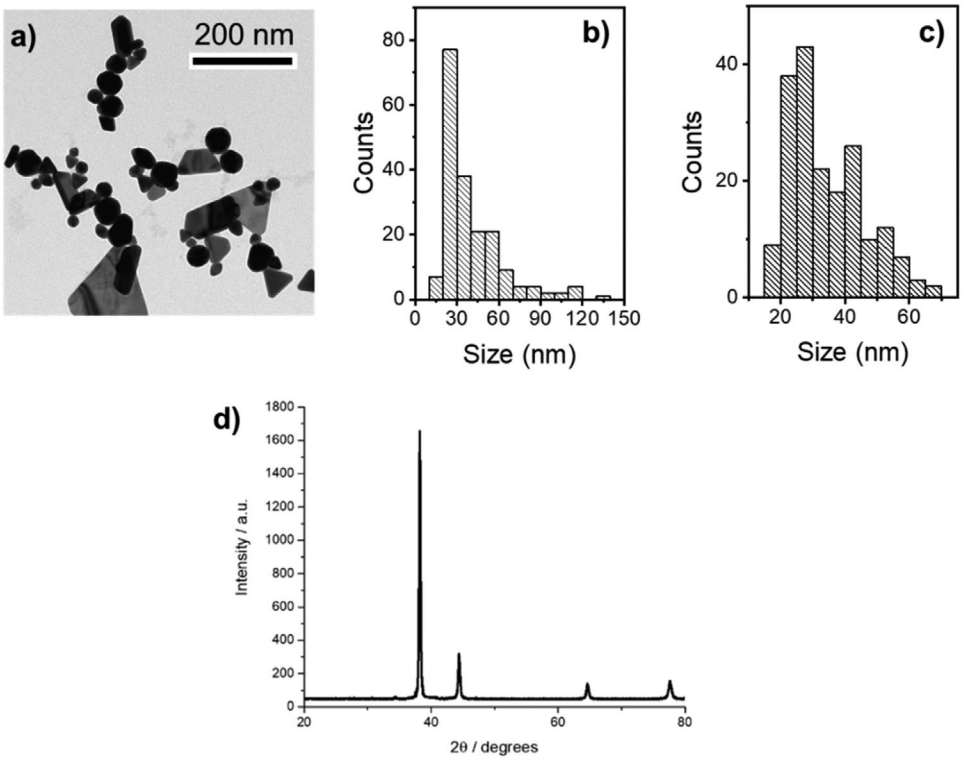

Figure 2. a) TEM images of the AuNS and size distribution of the b) triangular- and c) spherical-shaped nanoparticles. d) XRD pattern of the nanostructures. The four peaks are located at 38.1°, 44.3°, 64.5°, and 77.7°.

nanostructures as confirmed by the signals at high wavenumbers, in particular at 3250 and 3400 cm^{-1}.

ζ-potential measurement was performed for the AuNS capped by citric acid and a negative value of −38 mV is measured.

2.2. PBI/AuNS Deposition Procedure and Thin Films Characterization

The opposite electrostatic charges of the PBI and AuNS prompted us to immobilize the supramolecular adduct PBI/AuNS by means of a modification of the well-known layer-by-layer method.[35] The possibility to immobilize the adduct on a solid substrate is particularly interesting for applications in the field of sensors,[36] electronic and energy harvesting.[37] A hydrophobized substrate was dipped in a 1.5×10^{-4} M PBI chloroform solution with a dipping and withdrawal speed of 8 mm min^{-1}. The substrate was dried at room temperature for 30 min and then soaked in AuNS colloidal water suspension and pulled-out at a speed of 8 mm min^{-1}. The substrate was dried at room temperature for 30 min and then immersed in aqueous suspension of AuNS (0.2 g L^{-1}), withdrawn and dried at room temperature for 30 min and finally rinsed with ultrapure water to remove the excess of transferred AuNS.[22] The deposition process was monitored by means of quartz crystal microbalance (QCM): the resonant frequency changes

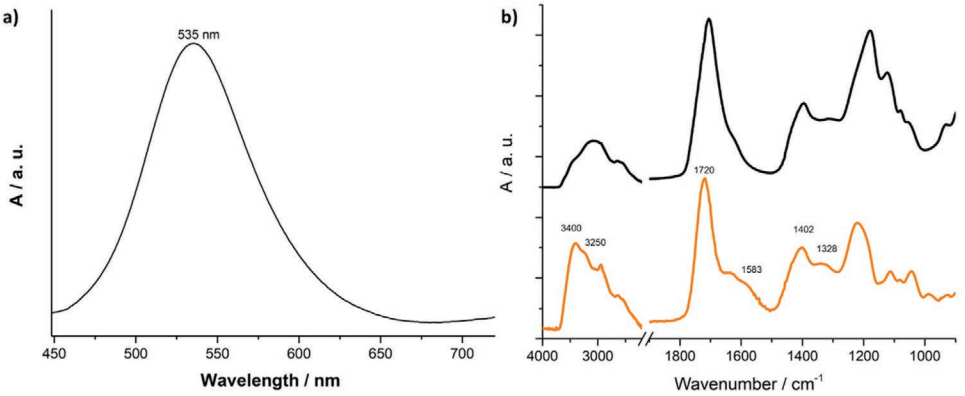

Figure 3. a) Visible spectrum of AuNS colloidal solution dispersed in water. b) FTIR spectra of citric acid (black line) and gold metallic nanostructures synthetized in presence of citric acid (orange spectrum) recorded on drop-cast films deposited on the ATR plate.

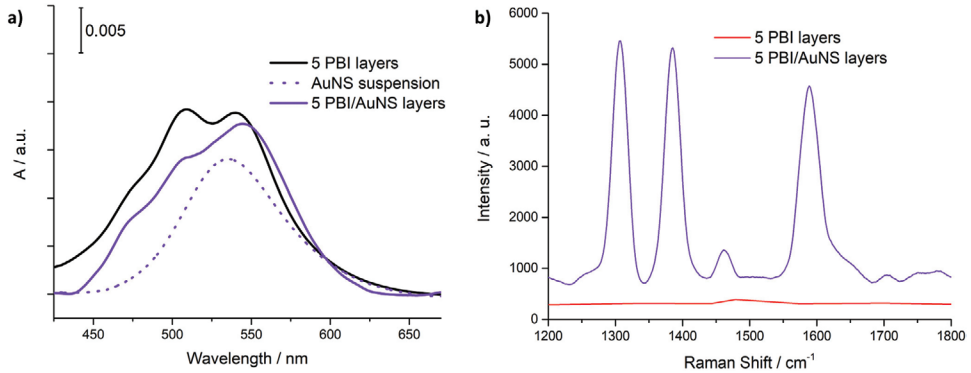

Figure 4. a) Visible spectra of 5 PBI layers (black line) and 5 PBI/AuNS layers (purple line) transferred on quartz slides. Visible spectrum of AuNS suspension is reported for clarity. b) Raman spectra of 5 PBI/AuNS layers and 5 dipping layers of PBI on silicon substrates.

recorded are directly proportional to the mass deposited on the microbalance,[38] and it was highlighted that the transfer process reaches a plateau after 5 PBI/AuNS layers (Figure S3, Supporting Information). The immobilized dyad was soaked in water to evaluate the desorption of the thin film (Figure S4, Supporting Information) confirming that the electrostatic interactions among the perylene bisimide and the metallic nanostructures ensure the thin film adhesion on the substrate.

Visible spectrum of five layers of PBI/AuNS film transferred on quartz substrates was recorded and compared with the five layers of PBI film transferred by dip-coating (**Figure 4**a). Visible spectrum of PBI film shows two signals located at 508 and 540 nm imputable to 0→1 and 0→0 vibronic band of $S_0 \rightarrow S_1$ transition in good agreement with the literature.[39] By investigating the A_{540}/A_{508} intensity ratio, the aggregation state of PBI molecules could be predicted.[40] PBI results mainly organized in H aggregates within the thin film, since the A_{540}/A_{508} value is below 0.9 (black line in Figure 4a).[41] The presence of metallic nanostructures influences the aggregation state of PBI with an inversion of intensity of such bands (purple line in Figure 4a) suggesting a slight change in the aggregates/monomers equilibrium in favor of the monomeric forms.

Raman spectroscopy was used to characterize the PBI and PBI/AuNS adduct transferred on silicon substrate (Figure 4b, red and purple lines, respectively). The typical signals of perylene bisimide core[42] at 1338, 1350, and 1592 cm^{-1} can be detected only in the presence of AuNS; a straightforward observation is the enhancement of the Raman signals of PBI in presence of the AuNS, characteristics of SERS effect.[43]

The Raman laser excitation wavelength centered at 532 nm is very close to localized surface plasmon resonance (LSPR) of AuNS at 535 nm promoting the energy transfer toward the attached molecule of PBI. The electrons of the metallic nanostructures are excited by the laser excitation source into a collective oscillation inducing the formation of an electromagnetic field at the metal–PBI interface and leading to the excitation of the molecules' polarizability.[44]

2.3. SPR Dopamine Detection by means of PBI/AuNS

It has been previously demonstrated that PBI derivatives can be used as active molecules for aromatic amines sensing.[22] Starting from these evidences, the effect of DA water solution on the Raman enhancement of PBI signals promoted by the AuNS has been tested. In fact, the Raman signals of PBI are remarkably reduced (Figure S5, Supporting Information) when DA water solution (10^{-9} M, concentration close to the physiological range[11]) is fluxed over five hybrid LbL layers of AuNS/PBI immobilized onto silicon slides. The rationale is the occurrence of chemical interactions among the plasmonic nanostructure and the PBI molecules. Furthermore, DA and PBI chemically interact and the mechanism can be supposed to be ruled by both dopamine amine group and PBI imide groups interaction and π–π interaction among DA aromatic ring and the perylene core.[22,45] According to the signals amplified in the Raman spectra, the vibrations of the perylene's core are influenced by the presence of DA molecules reducing their intensity.

SPR method[46,47] was used as transduction method for the development of an ultrasensitive platform able to detect DA in aqueous matrix. The effect of the AuNS on the surface plasmon propagation was evaluated by comparing the SPR curve of the slide covered with 5 PBI layers and that one covered by 5 LbL runs of PBI/AuNS. The variation of the ratio among the p-polarized (Rp) and s-polarized (Rs) reflected light (i.e., the light component with vibrating electric field parallel and perpendicular to the substrate, respectively) was monitored as a function of the light incident angle in the range of 58°–65°. A change in the minimum position of Rp/Rs suggest that the dielectric properties of the investigate surface are changing as a consequence of an interaction with an analyte and/or the presence of structures able to influence the surface plasmon propagation.[46]

Metal nanoparticles displaying a localized surface plasmon resonance have been indeed used to enhance the SPR response[48–50] and a change of the SPR energy is observed as a consequence of the coupling between the localized and the surface plasmons[26,27] with an angle shift of 1.76° toward larger angles in the presence of the AuNS (**Figure 5**, lines blue and orange, respectively). When AuNS are irradiated by photons with adequate energy the LSPR can be promoted and used as a probe for analytes detection,[43] furthermore an interfacial coupling among AuNS and the propagating plasmon on Au thin film (of SPR slide) can be promoted.[51,52] Different concentrations of DA were fluxed both on the PBI/SPR slide

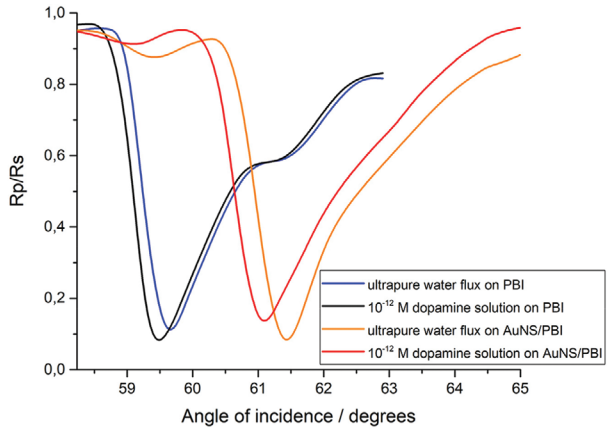

Figure 5. SPR curves of PBI under ultrapure water flux and 10^{-12} M DA water solution (blue and black lines, respectively). SPR curves of PBI/AuNS under ultrapure water flux and 10^{-12} M DA water solution (orange and red lines, respectively).

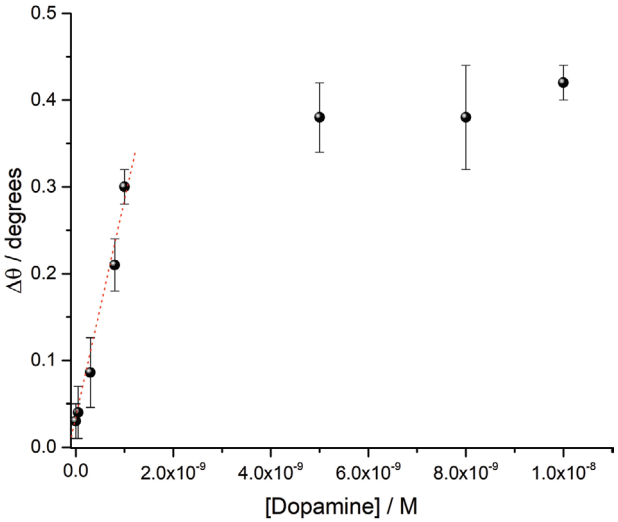

Figure 6. Shift of the plasmon angle for the SPR slide/PBI/AuNS active layer for CSF flux spiked with different DA concentrations.

and on PBI/AuNS/SPR slide. When 1×10^{-12} M DA solution is fluxed on the PBI deposited onto the SPR slide a shift of 0.16° (figure 5) was recorded. As already reported for SPR investigation of PBI derivatives and aromatic amines, when π–π interactions between the PBI core and the aromatic moiety of DA take place a shift toward smaller angles is observed.[22]

The presence of the AuNS strongly enhances the shift of the SPR angle that is twofold more intense if compared when only PBI is used as active molecule. In particular, a shift of 0.38° is observed when the PBI/AuNS adduct is used as the active layer (Figure 5).

The ability to detect DA was evaluated in aCSF prepared in laboratory (10×10^{-3} M glucose, 4×10^{-3} M sucrose, 2.5×10^{-3} M $CaCl_2$, 26×10^{-3} M $NaHCO_3$, 2×10^{-3} M $MgSO_4$, 2.5×10^{-3} M KCl, and 124×10^{-3} M NaCl[53]) and spiked with known concentrations of DA. DA levels in CSF can be thought as an important marker for diagnosis of neural diseases such as Parkinson's illness and Schizophrenia.[9] DA concentration range in physiological conditions is reported to be in the nanomolar range.[11] For this reason, it is particularly interesting the design of sensing devices with nanomolar sensitivity toward DA in this complex medium. In fact, CSF has a variegate composition, that can affect the measurement in terms of sensitivity and selectivity. In the presence of the interfering agents composing the CSF, in particular glucose, sucrose, and high salt concentration, the sensitivity of both PBI and PBI/AuNS active layers toward DA is strongly reduced and the angle shift is reduced by one order of magnitude in case of the PBI/AuNS adduct (Figure S6, Supporting Information), whilst no shift is detectable for PBI thin film. The DA concentration in CSF was investigated in the range of 10^{-8}–10^{-12} M. Shift of plasmon angle is reported in **figure 6**: a linear relation between the angle shift ($\Delta\theta$) and the DA concentration was recorded for low concentration values (10^{-12}–10^{-9} M) and an experimental limit of detection of 10^{-12} M has been obtained. For higher DA concentration, a response saturation is reached. At the best of our knowledge, picomolar sensibility represents one of the most performant results reported for DA optical sensing devices.[14,17]

3. Conclusion

AuNS with different morphologies (triangles, spheres, nanorods, etc.) have been ad hoc synthetized to be coupled with PBI derivatives within hybrid layers. AuNS are characterized by the localized plasmon resonance band at 535 nm; upon excitation at 532 nm, an effective energy transfer toward the PBI moieties happens, ensuring PBI Raman signals enhancement for SERS effect. Hence hybrid films, comprising a perylene bisimide derivative and Au nanostructures capped by citrate moieties, have been transferred onto silicon supports by a modified LbL approach. The SERS effect is interrupted in presence of DA (10^{-9} M); PBI Raman signal intensities strongly decrease, confirming the chemical interaction between DA and PBI. Additionally, both PBI alone and PBI/AuNS multilayers have been prepared directly onto the SPR supports. The hybrid layer exhibits a twofolded enhanced sensitivity (10^{-12} M) toward DA in aqueous solution suggesting the remarkable role played by AuNS. The proposed rationale for this improvement is the effective coupling of localized and surface plasmons. In fact, PBI/AuNS films have been used to detect dopamine in aCSF in the 10^{-12}–10^{-8} M range; a linear range of response (the SPR angle shift, $\Delta\theta$, vs DA concentration) between 10^{-12} and 10^{-9} M has been observed. The experimental limit of detection of 10^{-12} M is absolutely unusual and appealing even in comparison with other recent spectroscopic detection approaches for DA in complex fluids.[14,17] Therefore, the reported method is an innovative strategy for the real and effective implementation of a SPR based DA sensor.

4. Experimental Section

Materials and Methods: The PBI derivative was synthetized according to the procedure reported in the Supporting Information.

$HAuCl_4 \cdot 3H_2O$, citric acid monohydrate, $CHCl_3$, NaCl, D-glucose, sucrose, $CaCl_2$, $NaHCO_3$, $MgSO_4$, and KCl were purchased from Sigma-Aldrich and used without further purification. Ultrapure (type 1) water (18.2 MΩ cm at 25°) was used for all the experiments.

AuNS were investigated using a JEOL JEM-1011 microscope, working at an accelerating voltage of 100 kV, equipped by a high-contrast objective lens and a W filament electron source. Under these conditions, the ultimate point resolution of the microscope was equal to 0.34 nm. The TEM images were collected by a Gatan SC-1000 Orius Camera equipped with a fiber-optical coupled 11 MP CCD. The samples were prepared by casting a diluted drop of AuNS onto the 300 mesh amorphous carbon-coated Cu TEM grid, letting then the solvent to evaporate. Statistical analysis of the NS average size and size distribution was performed by using the freeware ImageJ analysis program.

UV–vis spectra of PBI solution, AuNS suspension, and thin films of PBI and Au/PBI adduct were recorded by a Lambda 650 spectrophotometer (Perkin Elmer). XRD analysis on AuNS was performed by a Bruker D2 PHASER diffraction from 20° to 80° with a step of 0.02°. Scan speed was fixed at 0.25° min^{-1}. As X-ray source a Cu Kα at 30 kV and 100 mA was used.

ζ-potential measurements were performed using a Malvern Panalytical Nano ZS Zetasizer instrument.

FTIR spectra were acquired by means of a Perkin Elmer Spectrum One spectrophotometer equipped with an ATR tool in the range of 4000–900 cm^{-1}. The infrared spectra (64 scans) of both citric acid and AuNS were recorded on the cast films of the compounds.

AuNS/PBI films were transferred on quartz, silicon/silicon dioxide, SPR slide, and quartz crystal microbalances. All the solid substrates were washed three times in water, acetone, and ethanol. The transfer process was performed by means of the LbL method:[35] the substrate, previously hydrophobized exposing the slide to hexamethyldisilazane vapor, was dipped in a chloroform PBI solution (1.5×10^{-4} M) and dried at room temperature for 30 min. Then, it was soaked in a water suspension of AuNS (0.2 g L^{-1}) and dried at room temperature for 30 min before being rinsed with ultrapure water.[22] The procedure was repeated to obtain multilayered films. For each deposition step, the immersion and emersion speeds were kept at 8 mm min^{-1}. Thin films of PBI were transferred from chloroform solution (1.5×10^{-4} M) by dip-coating method[54] with immersion/emersion speed of 8 mm min^{-1}.

The AuNS/PBI transfer process was monitored using a QCM: the resonant frequency of the QCM was measured by an openQCM Wi2 working at a resonance frequency of 10 MHz and the frequency variation was recorded after each deposition step.[55]

Raman spectra were recorded using a Horiba Xplora MicroRaman equipped with a 532 laser. The Raman spectra were acquired with a laser power of 0.125 mW cm^{-2}.

A nanofilm imaging ellipsometer (EP4) apparatus (Accurion) was used to perform SPR measurements. SPR substrates, 2×2 cm^2 SF-10 glass/Ti/Au slide (Ti and Au were thermal evaporated with a thickness of 2 and 50 nm, respectively, with a refractive index of 1.723 at 632.8 nm), were utilized for the SPR measurements. SF-10 index matching fluid, $n = 1.725$, was used to optically couple each interface. SPR measurement were acquired in the Kretschmann configuration with an incident light located at 632 nm monitoring the variation of the ratio among the p-polarized (Rp) and s-polarized (Rs) reflected light (Rp/Rs; i.e., the light component with vibrating electric field parallel and perpendicular to the substrate, respectively) in the light incident angle range comprised between 58° and 65° (0.01° as step). The different solutions were fluxed over the films by means of a peristaltic pump with a flux rate of 0.5 mL min^{-1} for ≈30 min. Then, in order to obtain the calibration curve SPR angle shift ($\Delta\theta$) versus DA molar concentration, $\Delta\theta$ values were calculated as the difference between the SPR angle of the active layer before and after the interaction with the analyte.

Synthesis of Au Nanostructures: Au nanostructures were synthetized by means of a chemical reduction method reported in the literature with some modifications.[56] More in detail, 100 mL of an aqueous solution of the $HAuCl_4{\cdot}3H_2O$ precursor and NaOH at a final concentration of 0.25×10^{-3} and 1×10^{-3} M, respectively, were put under stirring and heated until solution boiling was achieved. Then, 700 µL of a water solution of the citric acid reducing agent (2.5×10^{-3} M) were added, and the solution turns from transparent to purple; finally, the reaction solution was slowly cooled at room temperature in order to obtain the multishaped AuNS.[28]

Supporting Information

Supporting Information is available from the Wiley Online Library or from the author.

Acknowledgements

This research was supported by the PRIN 2017 (Protocol No. 2017PBXPN4_003), by the European Innovation Council through the INITIO-FET Project INITIO (Grant Agreement No. 828779), and by "Research for Innovation" POR PUGLIA FESR-FSE 2014/2020 Ricerca Regione Puglia.

Open access funding provided by Universita del Salento within the CRUI-CARE Agreement.

Conflict of Interest

The authors declare no conflict of interest.

Data Availability Statement

Research data are not shared.

Keywords

dopamine, gold nanostructures, perylene bisimide derivative, surface enhanced Raman spectroscopy, surface plasmon resonance

Received: June 18, 2021
Revised: August 31, 2021
Published online: September 29, 2021

[1] I. E. De Araujo, J. G. Ferreira, L. A. Tellez, X. Ren, C. W. Yeckel, *Physiol. Behav.* **2012**, *106*, 394.
[2] J. D. Berke, *Nat. Neurosci.* **2018**, *21*, 787.
[3] A. A. Grace, *Nat. Rev. Neurosci.* **2016**, *17*, 524.
[4] X. Ji, G. Palui, T. Avellini, H. Bin Na, C. Yi, K. L. Knappenberger, H. Mattoussi, *J. Am. Chem. Soc.* **2012**, *134*, 6006.
[5] A. Zhang, J. L. Neumeyer, R. J. Baldessarini, *Chem. Rev.* **2007**, *107*, 274.
[6] Y. Wang, Y. Zhang, C. Hou, M. Liu, *Microchim. Acta* **2016**, *183*, 1145.
[7] M. Senel, E. Dervisevic, S. Alhassen, M. Dervisevic, A. Alachkar, V. J. Cadarso, N. H. Voelcker, *Anal. Chem.* **2020**, *92*, 12347.
[8] M. Ouellette, J. Mathault, S. D. Niyonambaza, A. Miled, E. Boisselier, *Coatings* **2019**, *9*, 496.
[9] K. Syslová, L. Rambousek, V. Bubeníková-Valešová, R. Šlamberová, P. Novotny, P. Kacer, *Dopamine: Functions, Regulation and Health Effects*, Nova Science Publisher, New York **2012**.
[10] D. Caligiore, R. C. Helmich, M. Hallett, A. A. Moustafa, L. Timmermann, I. Toni, G. Baldassarre, *npj Parkinson's Dis.* **2016**, *2*, 16025.
[11] P. Li, B. Zhou, X. Cao, X. Tang, L. Yang, L. Hu, J. Liu, *Chem. –Eur. J.* **2017**, *23*, 14278.
[12] Z. Jinjin, C. Ming, Y. Caixia, T. Yifeng, *Analyst* **2011**, *136*, 4070.
[13] K. L. Davis, R. S. Kahn, G. Ko, M. Davidson, *Am. J. Psychiatry* **1991**, *148*, 1474.
[14] K. Zhang, Y. Liu, Y. Wang, R. Zhang, J. Liu, J. Wei, H. Qian, K. Qian, R. Chen, B. Liu, *ACS Appl. Mater. Interfaces* **2018**, *10*, 15388.
[15] V. D. Phung, W. S. Jung, T. A. Nguyen, J. H. Kim, S. W. Lee, *Nanoscale* **2018**, *10*, 22493.

[16] X. Yu, X. He, T. Yang, L. Zhao, Q. Chen, S. Zhang, J. Chen, J. Xu, *Int. J. Nanomed.* **2018**, *13*, 2337.
[17] A. Pathak, B. D. Gupta, *Biosens. Bioelectron.* **2019**, *133*, 205.
[18] W. Wang, C. H. Becker, H. Zhou, H. Lin, S. Roy, T. A. Shaler, L. R. Hill, S. Norton, P. Kumar, M. Anderle, *Anal. Chem.* **2003**, *75*, 4818.
[19] F. B. Kamal Eddin, Y. Wing Fen, *Sensors* **2020**, *20*, 1039.
[20] P. K. Badiya, V. Srinivasan, T. P. Jayakumar, S. S. Ramamurthy, *ChemPhysChem* **2016**, *17*, 2791.
[21] A. R. Sadrolhosseini, S. Shafie, Y. W. Fen, *Appl. Sci.* **2019**, *9*, 1497.
[22] S. Bettini, Z. Syrgiannis, R. Pagano, L. Dordević, L. Salvatore, M. Prato, G. Giancane, L. Valli, *ACS Appl. Mater. Interfaces* **2019**, *11*, 17079.
[23] J. Zhang, K. Liu, G. Wang, C. Shang, H. Peng, T. Liu, Y. Fang, *New J. Chem.* **2018**, *42*, 12737.
[24] M. Zhang, J. Shi, C. Liao, Q. Tian, C. Wang, S. Chen, L. Zang, *Chemosensors* **2021**, *9*, 1.
[25] R. Herizchi, E. Abbasi, M. Milani, A. Akbarzadeh, *Artif. Cells, Nanomed., Biotechnol.* **2016**, *44*, 596.
[26] P. K. Jain, X. Huang, I. H. El-Sayed, M. A. El-Sayed, *Acc. Chem. Res.* **2008**, *41*, 1578.
[27] C. F. Chen, S. Der Tzeng, H. Y. Chen, K. J. Lin, S. Gwo, *J. Am. Chem. Soc.* **2008**, *130*, 824.
[28] S. Shiv Shankar, S. Bhargava, M. Sastry, *J. Nanosci. Nanotechnol.* **2005**, *5*, 1721.
[29] S. Krishnamurthy, A. Esterle, N. C. Sharma, S. V. Sahi, *Nanoscale Res. Lett.* **2014**, *9*, 627.
[30] K. Sneha, M. Sathishkumar, S. Kim, Y. S. Yun, *Process Biochem.* **2010**, *45*, 1450.
[31] F. Liebig, R. M. Sarhan, C. Prietzel, A. Reinecke, J. Koetz, *RSC Adv.* **2016**, *6*, 33561.
[32] C. Gao, J. Vuong, Q. Zhang, Y. Liu, Y. Yin, *Nanoscale* **2012**, *4*, 2875.
[33] M. Alloisio, M. I. Martinez-Espinoza, G. Dellepiane, M. Maccagno, S. Thea, M. Ottonelli, *Mater. Chem. Phys.* **2020**, *242*, 122472.
[34] V. A. Suárez-Toriello, C. E. Santolalla-Vargas, J. A. De Los Reyes, A. Vázquez-Zavala, M. Vrinat, C. Geantet, *J. Mol. Catal. A: Chem.* **2015**, *404–405*, 36.
[35] R. Pagano, C. Ingrosso, G. Giancane, L. Valli, S. Bettini, *Materials* **2020**, *13*, 2938.
[36] A. Buccolieri, S. Bettini, L. Salvatore, F. Baldassarre, G. Ciccarella, G. Giancane, *Sens. Actuators, B* **2018**, *267*, 265.
[37] S. Bettini, R. Pagano, V. Bonfrate, E. Maglie, D. Manno, A. Serra, L. Valli, G. Giancane, *J. Phys. Chem. C* **2015**, *119*, 20143.
[38] G. Giancane, M. R. Guascito, C. Malitesta, E. Mazzotta, R. A. Picca, L. Valli, *J. Porphyrins Phthalocyanines* **2009**, *13*, 1129.
[39] Z. Chen, B. Fimmel, F. Würthner, *Org. Biomol. Chem.* **2012**, *10*, 5845.
[40] M. Burian, F. Rigodanza, H. Amenitsch, L. Almásy, I. Khalakhan, Z. Syrgiannis, M. Prato, *Chem. Phys. Lett.* **2017**, *683*, 454.
[41] S. Bettini, Z. Syrgiannis, M. Ottolini, V. Bonfrate, G. Giancane, L. Valli, M. Prato, *Front. Bioeng. Biotechnol.* **2020**, *8*, 160.
[42] M. Angelella, C. Wang, M. J. Tauber, *J. Phys. Chem. A* **2013**, *117*, 9196.
[43] R. Pagano, M. Ottolini, L. Valli, S. Bettini, G. Giancane, *Colloids Surf., A* **2021**, *624*, 126787.
[44] A. I. Pérez-Jiménez, D. Lyu, Z. Lu, G. Liu, B. Ren, *Chem. Sci.* **2020**, *11*, 4563.
[45] F. Candotto Carniel, L. Fortuna, D. Zanelli, M. Garrido, E. Vázquez, V. J. González, M. Prato, M. Tretiach, *J. Hazard. Mater.* **2021**, *414*, 125553.
[46] S. Bettini, R. Pagano, V. Borovkov, G. Giancane, L. Valli, *J. Colloid Interface Sci.* **2019**, *533*, 762.
[47] A. Colombelli, M. G. Manera, V. Borovkov, G. Giancane, L. Valli, R. Rella, *Sens. Actuators, B* **2017**, *246*, 1039.
[48] R. Antiochia, P. Bollella, G. Favero, F. Mazzei, *Int. J. Anal. Chem.* **2016**, *2016*, 2981931.
[49] L. He, E. A. Smith, M. J. Natan, C. D. Keating, *J. Phys. Chem. B* **2004**, *108*, 10973.
[50] S. Szunerits, J. Spadavecchia, R. Boukherroub, *Rev. Anal. Chem.* **2014**, *33*, 153.
[51] B. S., K. NCSS, C. S. P., R. S. S, *Langmuir* **2020**, *36*, 2865.
[52] A. Rai, S. Bhaskar, S. S. Ramamurthy, *ACS Appl. Nano Mater.* **2021**, *4*, 5940.
[53] R. A. De Toledo, M. C. Santos, E. T. G. Cavalheiro, L. H. Mazo, *Anal. Bioanal. Chem.* **2005**, *381*, 1161.
[54] S. Bettini, R. Pagano, L. Valli, G. Giancane, *Chem. - Asian J.* **2016**, *11*, 1240.
[55] P. Semeraro, Z. Syrgiannis, S. Bettini, G. Giancane, F. Guerra, A. Fraix, C. Bucci, S. Sortino, M. Prato, L. Valli, *J. Colloid Interface Sci.* **2019**, *553*, 390.
[56] L. Zhao, D. Jiang, Y. Cai, X. Ji, R. Xie, W. Yang, *Nanoscale* **2012**, *4*, 5071.